

25<sup>th</sup> ABCM International Congress of Mechanical Engineering  
October 20-25, 2019, Uberlândia, MG, Brazil

## COB-2019-0782

# NUMERICAL STUDY OF AN ICE THERMAL ENERGY STORAGE TANK FOR SMALL SCALE APPLICATIONS

### Thiago Torres Martins Rocha

Department of Mechanical Engineering, Federal University of Minas Gerais. Av. Presidente Antônio Carlos, 6627, Pampulha, CEP 31270901, Belo Horizonte, Minas Gerais, Brazil.

[thiagotorres.rocha@yahoo.com.br](mailto:thiagotorres.rocha@yahoo.com.br)

### Cleison Henrique de Paula

Department of Mechanical Engineering, Federal University of Minas Gerais. Av. Presidente Antônio Carlos, 6627, Pampulha, CEP 31270901, Belo Horizonte, Minas Gerais, Brazil.

[cleissonhp@yahoo.com.br](mailto:cleissonhp@yahoo.com.br)

### Iuri Tannus Mendes Torres

Department of Mechanical Engineering, Vila Velha University. Av. Comissário José Dantas de Melo, 21, Boa Vista, CEP 29102920, Vila Velha, Espírito Santo, Brazil.

[iuritmt@hotmail.com](mailto:iuritmt@hotmail.com)

### Tiago de Freitas Paulino

Federal Center of Technological Education of Minas Gerais. Av. Amazonas, 5253, Nova Suiça, CEP 30421169, Belo Horizonte, Minas Gerais, Brazil.

[tfpaulinoeng@gmail.com](mailto:tfpaulinoeng@gmail.com)

### Raphael Nunes de Oliveira

Department of Mechanical Engineering, Federal University of Minas Gerais. Av. Presidente Antônio Carlos, 6627, Pampulha, CEP 31270901, Belo Horizonte, Minas Gerais, Brazil.

[rphnunes@demec.ufmg.br](mailto:rphnunes@demec.ufmg.br)

**Abstract.** *Thermal energy storage (TES) has been a proven technology to help reducing the costs associated with the electricity consumption in refrigeration systems. Besides the typical large-scale applications (e.g. air conditioning in buildings), the TES demonstrated to be a useful tool even in relatively small systems, such as domestic refrigerators. In an ice TES system, the ice tank is one of the most important aspects to analyze. Many works have been made to evaluate the performance of such tanks, but considering big capacities (20-350 kWh). In the present study, an external melt ice-on-coil tank is proposed for small scale applications, with 2.5 kWh of thermal capacity. The charge process (ice formation) is numerically simulated in a commercial finite element software. To give the initial inputs, the process of water solidification around a single tube was analyzed. Then, based on the presented assumptions, the tank dimensions were established, considering the cost of materials usually employed. The model was checked comparing a simulation with another numerical study, but experimentally validated. The results for the tank simulation indicated the influence of the heat gain from ambient, as well as the interaction between neighboring tubes in the ice formation. The proposed model and the adopted methodology can be considered as a good approximation to study an ice-on coil tank for small scale applications.*

**Keywords:** *thermal energy storage, ice tank, small scale, simulation.*

## 1. INTRODUCTION

The energy management is a topic of great discussion and importance nowadays. In 2017, the Brazilian government raised the electricity tariff to the red color level 2, class of higher cost. Because of this and other issues, alternatives to reduce energy consumption have become more relevant. In this context, the thermal energy storage (TES), associated to thermal systems, represents an option to reduce the demand at peak times (Wu and Tsai, 2015) and to decrease the electricity bill. Besides, in some configurations, the TES may be able to reduce installation and operating costs when compared to conventional systems (Sebzali et al, 2014).

The TES technique consists of storing energy or absence of thermal energy over a period of time, to use at a different time. It is usually employed when the schedules of higher demand (peak) and the economically more favorable

supply do not match. TES systems used for cooling can be divided into two main groups: those based on sensible heat, including water, fluids for low temperature, thermal mass; and those based on latent heat, such as ice (ITES) and phase change materials (PCM). Ice is certainly a PCM, but this terminology is typically employed for eutectic salts, salt hydrates, greases, paraffins (Hyman, 2011). The ITES systems are generally categorized as: ice harvesting, ice-on-coil (internal or external), ice slurry and encapsulated ITES (Yau and Rismanchi, 2012).

In tropical countries such as Malaysia, air conditioning systems in commercial buildings can account for 57% of total electricity consumption. For this reason, the TES is widely used in these buildings, in hospitals, schools, churches (Rismanchi et al, 2013). But, despite the consolidated use in large facilities, researches reveal the potential of applying the TES in smaller systems. In two experiments involving domestic refrigerators, the integration of PCM's represented a saving of 12% in the electricity and an 8% increase in COP (Elarem et al, 2017), while Liu et al (2017) reached an 18.6% reduction in energy consumption. As can be seen, the TES applied to systems with lower thermal load is an effective way to reduce electricity expenses. Furthermore, another incentive factor to use the TES in Brazil is the creation of the white tariff, through Normative Resolution 733/2016 of ANEEL, which establishes differentiated tariffs at peak and off-peak times for residential consumers. Therefore, it becomes important to expand the studies for smaller refrigeration equipment.

One of the most important aspects, if not the most, in an ITES system is the ice tank. Many works have been developed to study the ice tank performance and the ice formation. Sang et al (2016) numerically simulated a full ice on coil tank with 70 kWh of thermal capacity. They analyzed the water phase change and experimentally validated the model, reporting a close agreement between numerical and experimental results. Navarro et al (2013) experimentally studied a commercial ice-on-coil tank with nominal capacity of 350 kWh. The temperature distribution of the water/ice, of the heat transfer fluid and the energy consumption was measured. They found that a low mass flow rate and colder supply temperatures of the heat transfer fluid conducted to a faster tank charging, with the lowest energy consumption. Mammoli and Robinson (2018) proposed and numerically analyzed an ice tank with 20 kWh of thermal capacity to be used in residential applications. They concluded that the proposed tank can outperform a battery system, even before any optimization. Jordan et al (2018) proposed and experimentally analyzed an ice tank with thermal capacity of 20.7 kWh (74,400 kJ), to be used for fast cooling in milk production. They observed the ice formation, temperature distribution and the refrigeration system capacity, concluding that the collected data showed good agreement with the model used to size the tank.

Although the ice tank performance has been numerically and experimentally studied by many researchers, the focus is given to relatively big installations. To the best of the author's knowledge, there are no published works analyzing an ice tank with declared capacity below 20 kWh. In this sense, based on the demonstrated potential to apply the TES in smaller systems and in the absence of small capacity ice tanks studies, this work aims to propose and to study the performance of the charge process in an external melt ice-on-coil tank with 2.5 kWh of thermal capacity. After proposing the physical model, the time-wise variation of ice, the interaction between adjacent ice layers and the surrounding impact on ice formation are investigated.

## 2. PROBLEM DESCRIPTION

An external melt ice-on-coil tank for small scale applications is proposed in this work. In order to give the initial inputs, the process of water solidification around a single tube was analyzed. Then, based on the defined thermal loads and other assumptions, the tank dimensions were established, considering the cost of common materials usually employed. To verify the model validity, the ice formation was compared with that of another numerical study, experimentally validated. Lastly, the performance of the chosen tank geometry was investigated.

### 2.1 Model assumptions

The water initial condition was considered as liquid state at 0 °C. Then, the only mechanism of heat transfer in water is conduction. The adopted material for the tube was copper, with internal and external diameters of 4.77 mm and 6.35 mm, respectively. The boundary conditions at the inside surface were considered to be a constant temperature of -10 °C.

The nucleation temperature in which the ice starts to form could be lower than 0 °C, i.e., the water can reach a certain degree of subcooling. Some factors that could contribute for this phenomenon are the water composition and the tube temperature. Navarro et al (2013) related that nucleation took place between -1 °C and -3.1 °C in a set of experiments. Grozdek et al (2010) reported -0.4 °C of subcooling in their experiment. In this work, no subcooling of water was assumed and the phase-change temperature is 273 K. Another effect that can occur is a temperature range, called mushy region, instead of a single temperature point of the phase-change. Ismail et al (2000) numerically simulated the ice formation around finned tubes. In most of simulations, they considered a temperature range of 0.1 °C, but also investigated the effect of enlarging the mushy region. It was found that the phase-change temperature range causes linear increase in time for water solidification. In the present work, was considered a temperature range of 0.1 °C.

A system with refrigerating capacity of 230 W, excluding losses, is analyzed. For a chilled water tank, the ASHRAE (ASHRAE, 2012) says that a well-designed tank has a volumetric efficiency of 90% or higher. However, a reference number for ice tanks was not found in the open literature. Even if the volumetric efficiency is not the same thing as insulation efficiency, a limit of 5% was chosen for the heat losses due to the thermal insulation. In this sense, a total cooling load, including all the thermal losses, was established as 250W. In the next section, this value will be verified.

The original refrigeration system (without ice tank) is supposed to operate during 10 hours in a day, and the operating strategy of ice tank is considered as full storage, i.e., the system should be completely turned off during this time and the cooling loads must be supplied exclusively by the ice tank. The total charging time (ice formation) was supposed to be 8 h. The total capacity of the tank (Q) is then 250W times the 10 hours of operation, corresponding to 2.5 kWh or 9000 kJ. The latent heat of fusion (L) is 334 kJ/kg and, thus, the approximately mass of ice (m), obtained by Eq. (1), is 27 kg.

$$Q = mL \quad (1)$$

## 2.2 Governing equations and boundary conditions

The phase-change phenomenon of water solidification (fusion) is a typical problem of moving-boundary. The solutions of such problems are inherently difficult and the exact results are limited to idealized situations e.g., infinite or semi-infinite regions with simple boundary and initial conditions (OZISIK, 1980). The case of a one-dimensional semi-infinite domain, known as Stefan's or Neumann's problem, in cylindrical coordinates, are shown in Fig. 1. This process is governed by Eq.'s (2), (3) and (4), for the liquid phase, solid phase and the interface, respectively. The initial and boundary conditions at inside surface, interface and at far away surface are given by Eq.'s (5)-(8), respectively.

$$\frac{1}{r} \frac{\partial}{\partial r} \left( k_l r \frac{\partial T_l}{\partial r} \right) = \rho c_{p,l} \frac{\partial T_l}{\partial t} \quad (2)$$

$$\frac{1}{r} \frac{\partial}{\partial r} \left( k_s r \frac{\partial T_s}{\partial r} \right) = \rho c_{p,s} \frac{\partial T_s}{\partial t} \quad (3)$$

$$-k_l \frac{\partial T_l}{\partial r} \Big|_{r=s(t)} + k_s \frac{\partial T_s}{\partial r} \Big|_{r=s(t)} = \rho_s L \frac{\partial s(t)}{\partial t} \quad (4)$$

$$T(r, t=0) = T_0 \quad (5)$$

$$T(r=r_1, t) = T_1 \quad (6)$$

$$T_l(r=s(t), t) = T_s(r=s(t), t) = T_{sl} \quad (7)$$

$$T(r \rightarrow \infty, t) = T_0 \quad (8)$$

where  $r$  is the radial dimension,  $k$  is the thermal conductivity,  $T$  is temperature,  $\rho$  is the density,  $c_p$  is the specific heat,  $t$  is time,  $L$  is the latent heat of fusion and  $s(t)$  is the radial dimension at phase-change interface. The indexes are:  $s$  for solid,  $l$  for liquid and  $sl$  for solid-liquid interface.

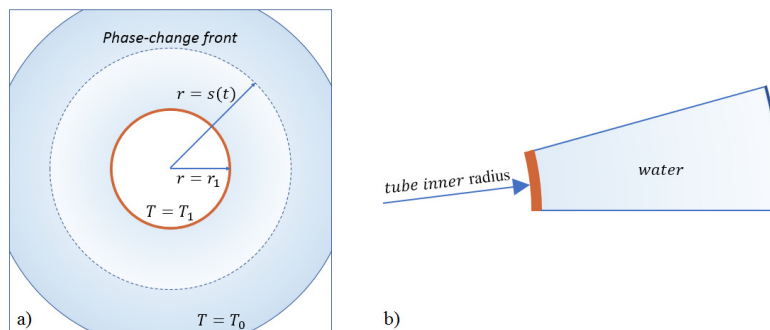


Figure 1. a) representation of Stefan's problem in cylindrical coordinates; b) geometry considered in the single tube simulation (not to scale).

These equations take in account only conduction as the heat transfer mechanism. If convection cannot be neglected, then it should be included in the liquid heat flux term.

### 2.3 Single tube analyses

To give a guideline to the tank geometry, the ice growth around a single tube immersed in water was verified. In this work, all the analyses of phase-change were performed in a commercial finite element software. To save computational time and due to the symmetric configuration, only a 1/360 fraction of the domain (Fig.1 b) was implemented, with the symmetry interfaces set as adiabatic. The thermophysical properties of copper and water are listed in Tab. 1, where T is temperature, Cp is the specific heat,  $\rho$  is density and k is the thermal conductivity.

Table 1. Thermal properties of copper and water.

WATER <sup>(1)</sup>				
T [k]	T [°C]	Cp [kJ/kg.K]	$\rho$ [kg/m <sup>3</sup> ]	k [W/m.K]
263	-10	1.997	918.1	2.320
268	-5	2.032	917.5	2.267
273 (solid)	0	2.066	917.0	2.216
273 (liquid)	0	4.217	999.8	0.569
275	2	4.211	999.9	0.574
COPPER <sup>(2)</sup>				
T [k]	T [°C]	Cp [kJ/kg.K]	$\rho$ [kg/m <sup>3</sup> ]	k [W/m.K]
200	-73	0.356	8933	413
300	27	0.385	8933	401

<sup>(1)</sup> properties of ice from Fukusako (1990); properties of water from Incropera et al (2008)

<sup>(2)</sup> Incropera et al (2008)

To check the grid convergence, the element size was gradually reduced until 0.05 mm, when the temperature in the control node stabilized in the third decimal. The timewise variation of ice can be seen in Fig. 2.

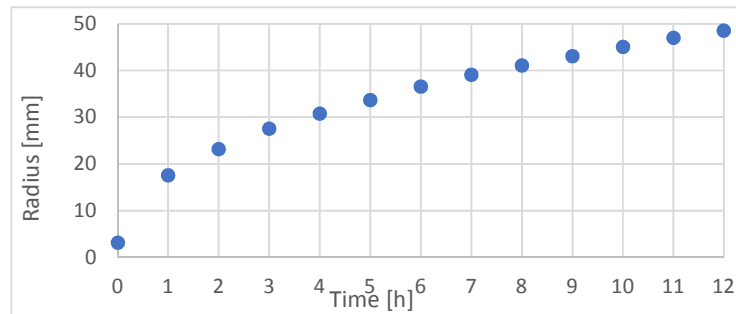


Figure 2. Ice evolution in a single tube.

### 2.4 Tank geometry and materials

Considering the mass of 27 kg, the charging time of 8 h and only one tube, the length of tank should be almost 5.5 m. Chosen a geometry with 7 tube passes, without interference between each other, the length is divided by 7, giving 780mm. To compute the U connections between tube passes, 25 mm will be added to the previous 780 mm. The tank cross section will have a regular hexagonal shape. Then, the tank internal dimensions are 805 x 131 mm (length x side), with a volume of 0.036 m<sup>3</sup>.

At this point, the thermal losses should be determined to verify the adequacy to the value of 250W of total cooling load. On the other hand, the losses depend on tank geometry and the materials choice. In this sense, common materials generally used in chilled or ice small capacity reservoirs were collected among manufactures. Polypropylene (PP) and stainless steel AISI 304 was found to be largely applied as the tank structure, while expanded polystyrene (EPS) and polyurethane (PU) are responsible for the insulation. The thermophysical properties and prices (in Brazilian reais) of these materials, are listed in Tab. 2 and 3, respectively. The price of the copper tube is US\$ 2.40/m. For temperature dependent thermal conductivity of PU and EPS, Zhang et al (2017) and Gnip et al (2012) can be use, respectively.

Table 2. Thermophysical properties of PP, AISI 304, EPS and PU.

PP <sup>(1)</sup>				
T [k]	T [°C]	Cp [kJ/kg.K]	DENS [kg/m <sup>3</sup> ]	k [W/m.K]
298	25	1.588	910	0.24
AISI 304 <sup>(2)</sup>				
T [k]	T [°C]	Cp [kJ/kg.K]	DENS [kg/m <sup>3</sup> ]	k [W/m.K]
200	-73	0.402	7900	12.6
300	27	0.477	7900	14.9
EPS <sup>(3)</sup>				
T [k]	T [°C]	Cp [kJ/kg.K]	DENS [kg/m <sup>3</sup> ]	k [W/m.K]
295	22	1.280	23	0.034
PU <sup>(3)</sup>				
T [k]	T [°C]	Cp [kJ/kg.K]	DENS [kg/m <sup>3</sup> ]	k [W/m.K]
295	22	1.537	33	0.022

<sup>(1)</sup> Sherey et al (2008); <sup>(2)</sup> Incropera et al (2008); <sup>(3)</sup> Al-Ajlan (2006);

Table 3. Prices of PP, AISI 304, EPS and PU boards/slabs.

Material	EPS			PU			AISI 304	PP
Thickness [mm]	40	50	60	25	30	50	1	3
Price <sup>(1)</sup> [US\$/m <sup>2</sup> ]	7.9	9.4	10.5	10.2	11.8	21.2	83,8	15.7

<sup>(1)</sup> All the prices are based on the Exchange rate of R\$ 1.00 = US\$ 3.82, on 11/23/18.

Initially, the materials selected would be PP for the tank structure and EPS for insulation, due to the lowest price. The thermal losses ( $q$ ) were estimated based on the concept of thermal resistance, Eq. (9), considering an inside temperature in PP board of 0 °C ( $T_{wall}$ ) and an ambient temperature in external surface of insulation material of 30 °C ( $T_{\infty}$ ). This temperature was considered due to the possibility of the tank proximity with the condenser or compressor of the refrigeration system. Besides, natural convection with a coefficient of 10 W/m<sup>2</sup>K ( $h$ ) was adopted in the outside surface.

$$q = \frac{T_{\infty} - T_{wall}}{\frac{1}{hA} + \frac{x_{PP}}{kA} + \frac{x_{ins}}{kA}} \quad (9)$$

where  $A$  is the corresponding area to each thermal resistance quota,  $x_{PP}$  and  $x_{ins}$  are the thicknesses of the PP board and insulation board, respectively. The expanded PU was also checked in case of EPS inadequacy. The thermal resistance ( $R$ ) and the losses are shown in Tab. 4, where the indexes (s), (e) and (total) stands for lateral side, ends and sum of lateral and ends, respectively.

Table 4. Thermal resistance and losses of PU and EPS boards with different thicknesses.

Material	Thickness [mm]	R(s) [m <sup>2</sup> .K/W]	R(e) [m <sup>2</sup> .K/W]	Heat loss(s) [W]	Heat loss(e) [W]	Heat loss(total) [W]	Heat loss(total) [%]
PU	30	2,07	1,48	14,51	2,81	17,32	7,4
PU	50	3,10	2,39	9,66	1,74	11,40	4,9
EPS	40	1,73	1,29	17,30	3,22	20,52	8,7
EPS	50	2,06	1,58	14,60	2,62	17,22	7,3
EPS	60	2,36	1,88	12,73	2,21	14,94	6,4

As can be seen from Tab. 4, the EPS, with any thickness, did not meet the requirement of 5% thermal losses. Besides, the only adequate option is PU with 50 mm thickness. Thus, the latter one is the material selected for the insulation. Sanaye and Shirazi (2013), simulating an ice thermal energy storage system, considered the thermal resistance of the ice tank equal to 1.98 m<sup>2</sup>K/W. This value indicates that the EPS and the PU with the listed thicknesses in Tab. 4 were chosen as good candidates. Then, all the tank materials and dimensions were established, and the final arrangement is illustrated in Fig. 3. The total materials cost, excluding manufacturing and assembling, was estimated in

US\$ 41.90. If a 6.5% heat loss were allowed, then the EPS with 60 mm could be chosen and, the tank cost would decrease to US\$ 32.70.

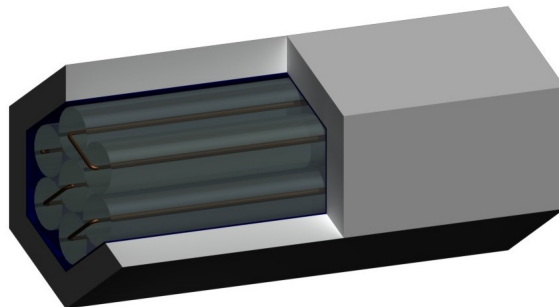


Figure 3. Final tank arrangement, with a cut on PP and PU layers to better show the tube bank.

### 3. TANK NUMERICAL MODEL

#### 3.1 Tank simulation

For the tank simulation, a few more assumptions were made. Although the effect of density variation was included in model, the level variation of water in tank during the ice building was not considered. In fact, as the ice grows, the level of water tends to rise and, when the tank is full, the pressure increases. Nevertheless, this can be easily managed by installing a simple control mechanism, keeping the water level and pressure constants. It was considered yet that the effect of the U connections between tubes is negligible.

After these considerations, the geometry was simulated to verify the possible interference between ice formation around the multiple tubes, as well as the influence of ambient conditions and construction materials. To save computational time and due to the symmetric shape, only a 1/12 fraction of the geometry was implemented, as can be seen in Fig. 4 a). The boundary conditions are the same as mentioned before for the single tube. However, the previous simulation did not include the tank construction materials, thus, the initial conditions at these regions must now be specified. To provide a reasonable estimate, the model was run to obtain the results of the steady-state temperature gradient, to be used as input for the initial conditions on tank simulation. In this case, the temperature of  $-10\text{ }^{\circ}\text{C}$  at the tube inside surface was disregarded and the temperature of liquid water was kept constant at  $0\text{ }^{\circ}\text{C}$ , with an ambient temperature of  $30\text{ }^{\circ}\text{C}$  and  $h=10\text{ W/m}^2\cdot\text{K}$ .

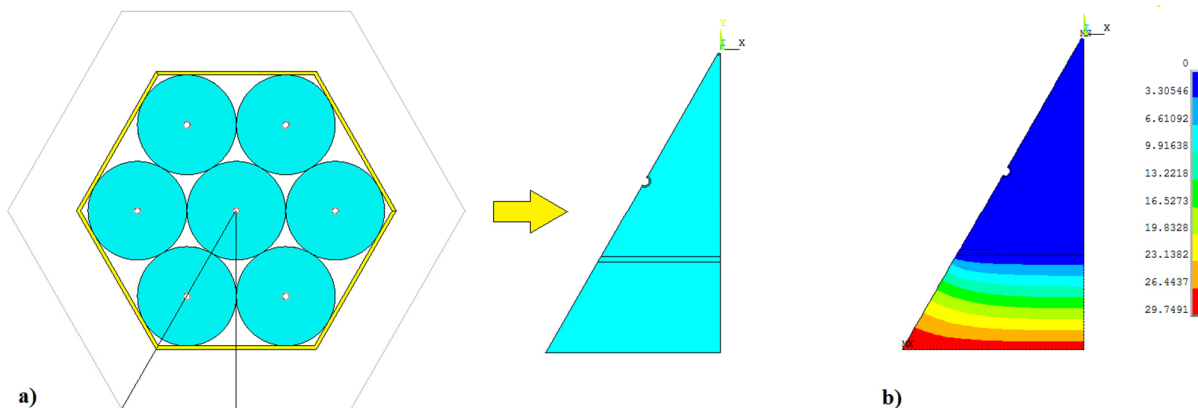


Figure 4. a) fraction of geometry simulated; b) result of steady-state temperature distribution.

#### 3.2 Model validation

To check the validity of the present model, the water solidification around one tube immersed in an insulated cavity was investigated. All the conditions were kept the same as studied by Sasaguchi et al (1997), including cylinder diameter of 25.4 mm, cylinder wall temperature of  $-10\text{ }^{\circ}\text{C}$  and initial temperature of  $0\text{ }^{\circ}\text{C}$ . Their model was experimentally validated for an initial temperature of  $4\text{ }^{\circ}\text{C}$  and, as reported, the predicted interface and the solid volume ratio were in excellent agreement with experimental data in the entire time range. The timewise variation of the volume

ratio, defined as the ratio of the solidified area ( $A_s$ ) to the total cross-sectional area of the cylinder ( $A_c$ ), was plotted for their (Sasaguchi et al, 1997) model and the present model. The results are show in Fig. 5.

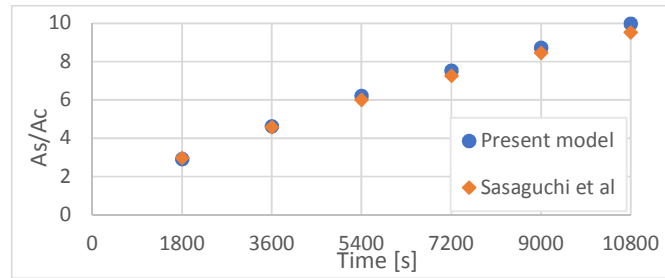


Figure 5. Timewise variation of the volume ratio presented by Sasaguchi et al (1997) and by the present study.

As can be seen in Fig. 4, the volume ratio predicted by the present model showed a good proximity with the values presented by Sasaguchi et al. Therefore, it can be assumed that the proposed model is valid to simulate the ice formation in more complex geometries, as that from this study.

#### 4. RESULTS AND DISCUSSION

The steady-state result is presented in Fig. 4 b). The temperature distribution in the PP board showed a tiny gradient, ranging from 0 °C to 0.6 °C. This indicates that a temperature dependent thermal conductivity for PP would not bring an improvement for the model. However, in PU insulation, the temperature ranged from 0.6 °C to almost 30 °C, hence, the effect of temperature dependent thermophysical properties could be verified in future works. Regarding the ice tank simulation results, Fig. 6 shows the temperature distribution at time intervals of 3600 s, 7200 s, 10800 s, 14400 s, 18000 s, 21600 s, 25200 s and 28800 s.

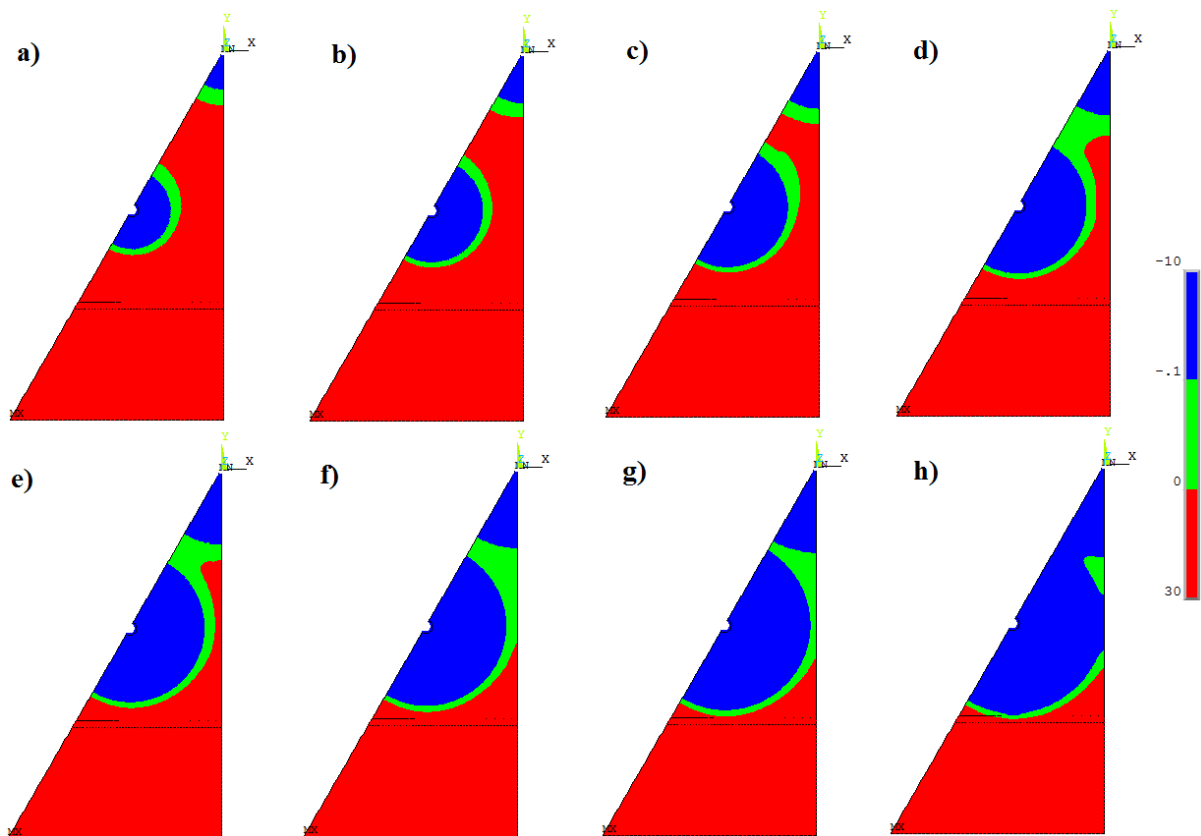


Figure 6. Temperature distribution at: a) 3600 s; b) 7200 s; c) 10800 s; d) 14400 s; e) 18000 s; f) 21600 s; g) 25200 s; h) 28800 s.

As the phase-change was set to occur in a range of 0.1 °C, a mushy zone was formed, represented by the green region (in the web version). After reaching -0.1 °C, the water is completed solidified and the ice fraction can be observed by the blue region (in the web version). In the single tube simulation, the ice is formed completely symmetric around the tube. In this case, the heat gain from the ambient influenced the ice formation, mainly at the bottom tube, where the mushy zone is not totally uniform. Besides, the ice fraction in the proximity of the PP board is a little bit lower than that of the single tube. However, this effect does not represent a major concern if the thermal insulation is well designed, as in this study.

Another important aspect to evaluate is the interaction between neighboring tubes. Until 25200 s (7 h) is not clearly possible to identify any profile alteration. However, at 28800 s (8 h), the linkage is evident between the external tubes and, even with the central tube, an interaction has occurred. In both cases, the interaction between tubes resulted in more ice formation than that observed in the single tube simulation.

## 5. CONCLUSIONS

An external melt ice-on-coil tank proposed to be used in small scale applications, with thermal capacity of 2.5 kWh, was investigated. In order to give an initial guess on tank geometry definition, the ice formation around a single tube was simulated. The results were used as input to define the tank dimensions. Different materials and thicknesses were pre-selected as the insulation candidates. However, only expanded PU with 50 mm thickness attended the 5% limit of thermal losses. To check the validity of the present model, a simulation was carried out in the same conditions considered by Sasaguchi et al (1997) and the results showed a good agreement with their data, validating the proposed model.

After establishing the tank arrangement, a simulation was carried out to verify the influence of the ambient and the impact of neighboring tubes. The results showed that the heat gain from ambient promoted a little reduction in the ice fraction formed at the bottom tube, but this decrease does not represent a major problem in case of well-designed thermal insulations. Furthermore, it was observed that the mushy zone formed around the bottom tube was not completely uniform, as was the case in the single tube analyze. Another point to mention is the interaction between neighboring tubes. This effect could be verified in all tube interfaces and has always occurred in the sense to form more ice when compared to the single tube. Based on the above considerations, the proposed model and the adopted methodology can be considered as a good approximation to study a melt ice-on coil tank for small scale applications.

## 6. ACKNOWLEDGEMENTS

The authors appreciate the support of the following Brazilian research financing institutions: CAPES, CNPq and FAPEMIG.

## 7. REFERENCES

- AL-AJLAN, Saleh A. *Measurements of thermal properties of insulation materials by using transient plane source technique*. Applied Thermal Engineering, Elsevier. 2006, Vol. 26, p. 2184-2191.
- ELAREM, R. et al. *Performance analysis of a household refrigerator integrating a PCM heat exchanger*. Applied Thermal Engineering, Elsevier. 2017, Vol. 125, p. 1320-1333.
- FUKUSAKO, S. *Thermophysical properties of Ice, Snow, and Sea Ice*. International journal of Thermophysics. 1990, Vol. 11, p. 353-372.
- GNIP, Ivan. et al. *Thermal conductivity of expanded polystyrene (EPS) at 10 °C and its conversion to temperatures within the interval from 0 to 50 °C*. Energy and Buildings, Elsevier. 2012, Vol. 52, p. 107-111.
- GROZDEK, Marino et al. *Development of a computer program for the simulation of ice-bank system operation, part II: Verification*. International Journal of Refrigeration, Elsevier. 2010, Vol. 33, p. 1657-1669.
- HYMAN, Lucas B. *Sustainable Thermal Storage Systems: Planning, Design and Operations*. McGraw-Hill, 2011.
- INCROPERA, Frank P. et al. *Fundamentals of heat and mass transfer*. John Wiley & Sons, 6th ed. 2007.
- ISMAIL, K. A. R. et al. *Ice formation around isothermal radial finned tubes*. Energy and Conversion Management, Elsevier. 2000, Vol. 41, p. 585-605.
- JORDAN, Rodrigo A. et al. *Modeling and testing of an ice bank for milk cooling after milking*. Engenharia Agrícola. 2018, Vol. 38, p. 510-517.
- LIU, Zhongbao et al. *Performance study on air-cooled household refrigerator with cold storage phase change materials*. International Journal of Refrigeration, Elsevier. 2017, Vol. 79, p. 130-142.
- MAMMOLI, Andrea; ROBINSON, Matthew. *Numerical analysis of heat transfer processes in low-cost, high-performance ice storage device for residential applications*. Applied Thermal Engineering, Elsevier. 2018, Vol. 138, p. 453-463.

- NAVARRO, A. López et al. *Experimental investigation of the temperatures and performance of commercial ice-storage tank*. International Journal of Refrigeration, Elsevier. 2013, Vol. 36, p. 1310-1318.
- OZISIK, M. Necati. *Heat conduction*. John Wiley & Sons, 1980.
- RISMANCHI, B. et al. *Modeling and simulation to determine the potential energy savings by implementing cold thermal energy storage system in office buildings*. Energy Conversion and Management, Elsevier. 2013, Vol. 75, p.152-161.
- SANAYE, Sepehr; SHIRAZI, Ali. *Four E analysis and multi-objective optimization of an ice thermal energy storage for air-conditioning applications*. International Journal of Refrigeration, Elsevier. 2013, Vol. 36, p. 828-841.
- SANG, Woo Hong et al. *Efficient numerical approach for simulating a full-scale vertical ice-on-coil latent thermal storage tank*. International communications in Heat and mass transfer, Elsevier. 2016, Vol. 78, p. 29-38.
- SASAGUCHI, K. et al. *A numerical analysis of the solid-liquid phase-change heat transfer around a single and two horizontal, vertically spaced cylinders in a rectangular cavity*. International journal of Heat and mass transfer, Elsevier. 1997, Vol. 40, p. 1343-1354.
- SEBZALI, M. J. et al. *Comparison of energy performance and economics of chilled water thermal storage and conventional air-conditioning systems*. Energy and Buildings, Elsevier. 2014, Vol. 69, p. 237-250.
- SHERELY, Annie Paul et al. *Effect of loading and chemical treatments on thermophysical properties of banana/polypropylene commingled composite materials*. Composites: Part A, Elsevier. 2008, Vol. 39, p. 1582-1588.
- WU, Chung-Tai; TSAI, Yao-Hsu. *Design of an ice thermal energy storage for a building of hospitality operation*. International Journal of Hospitality Management, Elsevier. 2015, Vol. 46, p. 46-54.
- YAU, Y.H; RISMANCHI, Behzad. *A review on cool thermal storage technologies and operating strategies*. Renewable and Sustainable Energy Reviews, Elsevier. 2012, Vol. 16, p.787-797.
- ZHANG, Hu. et al. *Experimental study of the thermal conductivity of polyurethane foams*. Applied Thermal Engineering. Elsevier. 2017, Vol. 115, p. 528-538.

## 8. RESPONSIBILITY NOTICE

The authors are the only responsible for the printed material included in this paper.